Journal of Physics: Conference Series **769** (2016) 012004 doi:10.1088/1742-6596/769/1/012004

Radio-interferometric and near-IR observations of PSR J1357−6429

Aida Kirichenko[1], Dmitry Zyuzin[1], Yury Shibanov[1,2], Peter Shternin[1], Andrey Danilenko[1], Sergey Zharikov[3], Maxim Voronkov[4], Dmitry Barsukov[1,2] and Ronald Mennickent[5]

[1]Ioffe Institute, 26 Politekhnicheskaya st., St. Petersburg 194021, Russia
[2]Peter the Great St. Petersburg Polytechnic University, 29 Politekhnicheskaya st., St. Petersburg 195251, Russia
[3]Observatorio Astronómico Nacional SPM, Instituto de Astronomía, Universidad Nacional Autónoma de Mexico, Ensenada, BC, Mexico
[4]CSIRO Astronomy and Space Science, Australia Telescope National Facility, PO Box 76, Epping, NSW 1710, Australia
[5]Department of Astronomy, Universidad de Concepcion, Casilla 160-C, Concepcion, Chile

E-mail: aida.astro@mail.ioffe.ru

Abstract. PSR J1357−6429 is a young radio pulsar detected in X-rays and γ-rays. We performed radio-interferometric and high spatial resolution near-infrared observations of the pulsar. Based on the obtained radio data, we estimated the most accurate pulsar position, RA = 13:57:02.525(14) and Dec = 64:29:29.89(15). Using the new and archival radio data, we obtained the 90 per cent pulsar proper motion upper limit $\mu < 106$ mas yr^{-1}, which corresponds to the pulsar transverse velocity $v_{tr} \lesssim 1300$ km s^{-1}. The near-infrared imaging revealed a point source which we propose as a pulsar near-infrared counterpart candidate. It is confidently detected in the J and K_s bands, with $J = 23.51\pm0.24$ and $K_s = 21.82\pm0.25$. The respective dereddened near-infrared fluxes are compatible with the long-wavelength extrapolation of the pulsar X-ray spectrum. If the candidate is the true counterpart, by this property PSR J1357−6429 would be similar to the nearby middle-age pulsar PSR B0656+14. In this case, both pulsars demonstrate an unusually high near-infrared efficiency relative to the X-ray efficiency as compared to other pulsars detected in both ranges.

1. Introduction

PSR J1357−6429 is a young (characteristic age $\tau = 7.3$ kyr) and energetic (spin-down luminosity $\dot{E} = 3.1 \times 10^{36}$ ergs s^{-1}) 166 ms pulsar [1]. At a distance of 2.5 kpc, estimated from its dispersion measure [1], it is one of the nearest young pulsars known. The pulsar is visible in X-rays, where it powers a tail-like pulsar wind nebula. A fainter pulsar plerion extended up to a few tens of arcminutes is detected in the X-ray, TeV and radio domains [2–6].

The optical source detected at the pulsar X-ray positions with the ESO Very Large Telescope (VLT) in 2009 was proposed as a pulsar optical counterpart candidate [7]. However, the candidate demonstrated a 5σ offset from the pulsar radio-interferometric position measured with the Australia Telescope Compact Array (ATCA) in 2000 [1]. The offset implied that the pulsar should have a very high transverse velocity of ≈ 2000 km s^{-1} assuming the distance of

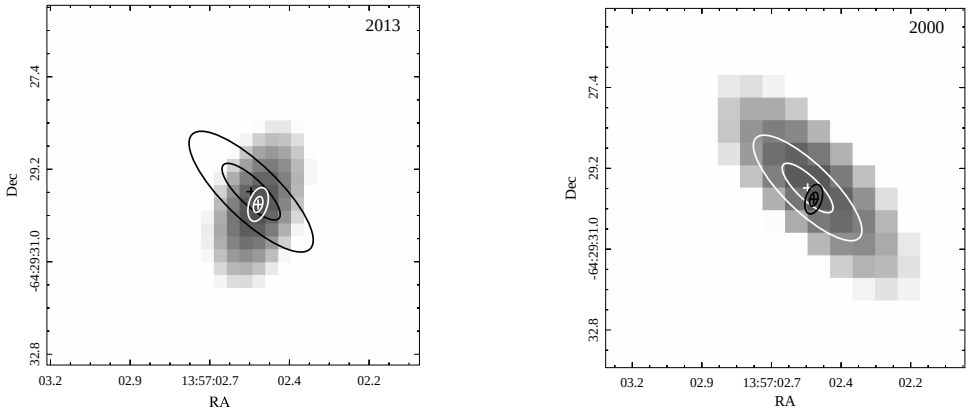

Figure 1. $8'' \times 8''$ ATCA image fragments with PSR J1357−6429 in the centre obtained in the 2013 (*left*) and 2000 (*right*) epochs with pixel scales of $0\overset{''}{.}25$ and $0\overset{''}{.}5$, respectively. For a given epoch, the derived pulsar position and the 40 and 90 per cent position uncertainties are shown by the white cross and ellipses, while the black cross and ellipses are related to the other epoch. The images were used for absolute astrometry.

2.5 kpc [7]. A similar estimate was obtained based on the difference between the pulsar radio and X-ray positions [8].

In order to verify the pulsar nature of the optical source and check if its velocity is indeed that high, we repeated the radio-interferometric observations with the ATCA and obtained near-infrared (IR) observations of the pulsar field using high spatial resolution techniques available at the VLT. We also performed an independent analysis of the archival radio-interferometric data obtained with the ATCA in 2000 [1].

For details of all observations, data reduction and analysis, see Refs. [9] and [10].

2. Radio-interferometric observations

We observed PSR J1357−6429 with the ATCA in 2013. Standard data reduction including Radio Frequency Interference (RFI) flagging, calibration and imaging was performed on the data with the `MIRIAD` package [11]. The data were obtained in the 1.078−3.126 GHz range. To account for a possible bias between the frequencies in the astrometrical analysis, we divided the total 2.048 GHz bandwidth into four 512 MHz sub-bands, which were analysed separately. The total bandwidth for the data obtained from the ATCA 2000 observations is 128 MHz. Given the narrower band as compared to the 2013 data, no splitting was applied to the 2000 data.

We obtained the resulting mean coordinates for the pulsar position in the ATCA 2013 data, RA = 13:57:02.525(14) and Dec = −64:29:29.89(15) (J2000). The derived position appears to be different from the previously reported values RA = 13:57:02.43(2) and Dec = −64:29:30.2(1) based on the ATCA 2000 observations [1] implying that the pulsar has moved between 2000 and 2013 epochs. To check the pulsar shift significance, we remeasured the pulsar position on the reprocessed ATCA 2000 data. The derived coordinates are RA = 13:57:02.546(76) and Dec = −64:29:29.64(55). The position uncertainties appear to be considerably larger than the reported ones (see Ref. [1]). As our uncertainties are consistent with the estimate based on the synthesised beam size and the pulsar signal-to-noise ratio (S/N), we conclude that the published pulsar position errors [1] were severely underestimated (see Ref. [9] for details).

In Fig. 1, we show the pulsar full-band images obtained for two epochs. The pulsar positions for the two observational epochs with the respective error ellipses at 40 and 90 per cent confidence levels are overlaid on the images. No significant pulsar shift is visible and only an upper limit of $\approx 1\overset{''}{.}3$ (90 per cent confidence) can be established.

To reliably determine the proper motion, we employed a more robust technique of relative

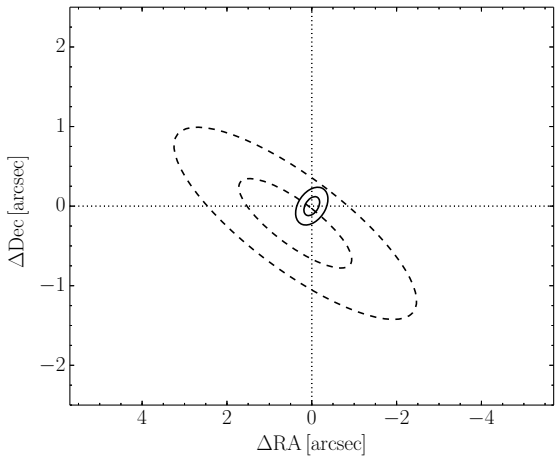

Figure 2. 40 and 90 per cent pulsar position uncertainty ellipses after relative astrometry. The 2013 and 2000 positions are shown by solid and dashed ellipses, respectively. The positions are shown relative to the mean pulsar position at the 2013 epoch. The offsets differ from those presented in Fig. 1 for the absolute astrometry (see text for details).

astrometry. We used the four sub-band images and one full-band image from the 2013 and 2000 data sets, respectively. The five images were aligned together using a custom-built routine. For referencing, we used nine bright point-like sources detected in all images with the S/N $\gtrsim 30$.

In Fig. 2, the mean of the pulsar positions in the aligned 2013 sub-bands is compared with the 2000 position. We find that the arrangement of the pulsar error ellipses on epochs 2000 and 2013 slightly differs from that provided by the absolute astrometry (cf., Fig. 1), while the pulsar shift is insignificant and its upper limit is virtually the same as obtained by the absolute astrometry (see Ref. [9] for details). Accounting for the time-base of 12.76 yr between the two ATCA observations, the 90 per cent upper limit on the pulsar proper motion is $\mu < 106$ mas yr^{-1}. It corresponds to the pulsar transverse velocity $v_{tr} \lesssim 1300$ km s^{-1} for the distance of 2.5 kpc.

3. Near-IR observations: a counterpart candidate

The first near-IR observations of the pulsar field were performed in the J, H and K_s bands with the Nasmyth Adaptive Optics System (NAOS) and Coude Near-Infrared Camera (CONICA) (in short NaCo) at the VLT/UT4 unit in the period of 2012–2013.

High spatial resolution provided by the adaptive optics system allowed us to find a pulsar near-IR counterpart candidate labelled by C' in Fig. 3. It overlaps with the pulsar position based on the ATCA 2013 observations (solid-line ellipse in the K_s-band image) and with the 1σ error ellipses of the pulsar X-ray positions obtained from the *Chandra* 2005 and *Chandra* 2009 observations (dashed-line ellipses in the K_s-band image). The source coordinates are RA=13:57:02.52 and Dec=−64:29:30.15. Its 1σ uncertainty for both coordinates is $0\farcs22$ in the K_s band. The object is detected with $J = 23.51\pm0.24$ and $K_s = 21.82\pm0.25$. There is also a hint of the source in the H band, but the full width at half maximum is worse by a factor of 1.5 in this band, meaning that a confident detection cannot be made. The candidate is unresolved from bright stars labelled A and A' in the previous seeing-limited VLT optical images [7].

One of the ways to support the pulsar nature of the candidate is to compare its colours with those of ordinary stars. However, such analysis appeared to be uninformative in our case, since $J - K_s$ colour of the object C' does not appear peculiar and is compatible with those of the

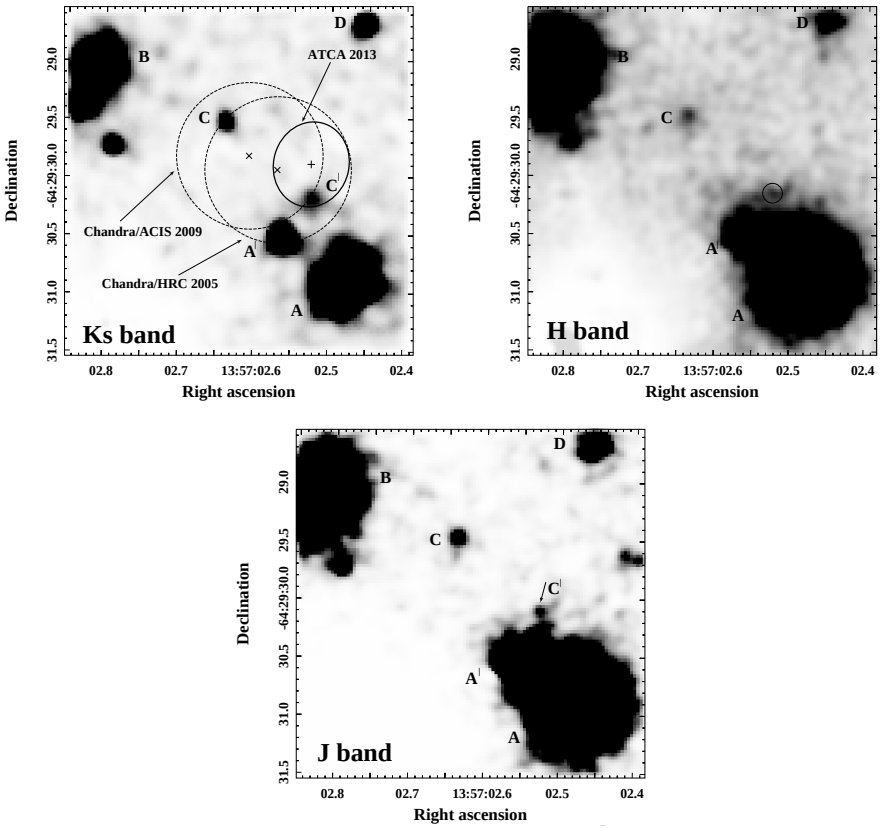

Figure 3. Image fragments of PSR J1357−6429 field obtained with the VLT/NaCo in K_s (*top-left*), H (*top-right*) and J (*bottom*) bands. The ×-points with dashed-line circles and the + with the solid-line ellipse in the *top-left* panel show the pulsar positions and their 1σ uncertainties from the two *Chandra* X-ray and new ATCA radio observations, respectively. A, A', B, C and D label objects as in [7]. C' labels the pulsar new counterpart candidate.

the M−L-dwarf sequence. The same property is found for other pulsars such as Crab, Vela and PSR B0540−69 (see Ref. [10] for details).

Another possibility to establish the C' nature is to compare its IR fluxes with the pulsar X-ray spectral data. As seen from Fig. 4, the near-IR fluxes of the counterpart candidate are consistent within 1σ uncertainties with the long-wavelength extrapolation of the pulsar X-ray spectrum. The same situation is observed for the middle-aged pulsar B0656+14 [12, 13].

We also performed the analysis of spindown power conversion efficiencies to the X-ray and K_s-band emission for the pulsars detected in both ranges. The efficiencies are defined as $\eta_X \equiv L_{\rm X}/\dot{E}$ and $\eta_{K_s} \equiv L_{K_s}/\dot{E}$, where $L_{\rm X}$ and L_{K_s} are the X-ray (0.5−8 keV) nonthermal and K_s luminosities, respectively. The plot in Fig. 5 demonstrates a strong correlation between Log η_{K_s} and Log η_X. The only pulsar, which shows an excess of the near-IR efficiency over the fit, is PSR B0656+14. It was discussed that the excess could point to the presence of a passive post-supernova fall-back disk around the pulsar [13]. However, it could also represent an intrinsic property of the pulsar magnetospheric emission. If the object C' is confirmed as the PSR J1357−6429 near-IR counterpart, it will be another example of a pulsar with a peculiar near-IR efficiency. This is important for understanding the origin of the near-IR and optical emission of pulsars.

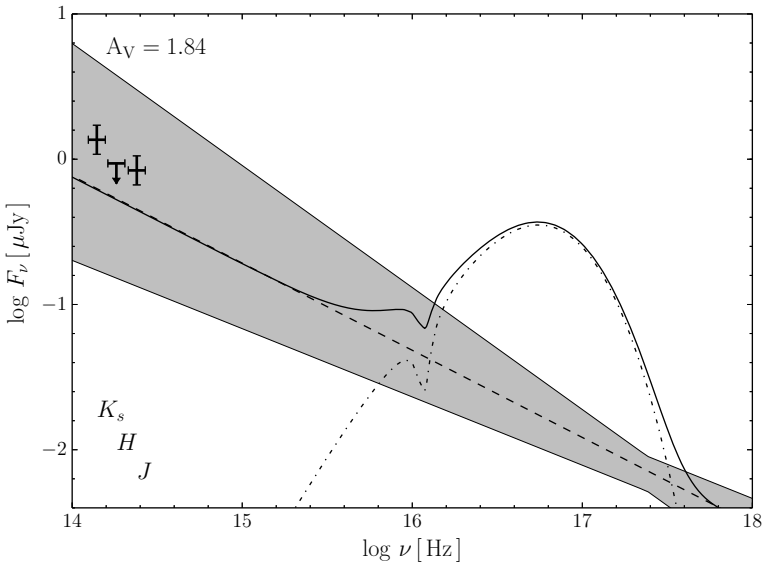

Figure 4. Tentative multi-wavelength unabsorbed spectrum of PSR J1357−6429. The X-ray part is described by the magnetized NS hydrogen atmosphere and power law models and is taken from [7]. The solid, dash-dotted and dashed lines are the total X-ray spectrum and contributions of the atmospheric and power law components, respectively. The grey region shows uncertainties of the power law component. The X-ray spectrum is extrapolated to the near-IR. The JK_s fluxes and the H-band upper limit for the object C' dereddened with the plausible extinction value A_V [7] presented in the plot are shown by bold error bars.

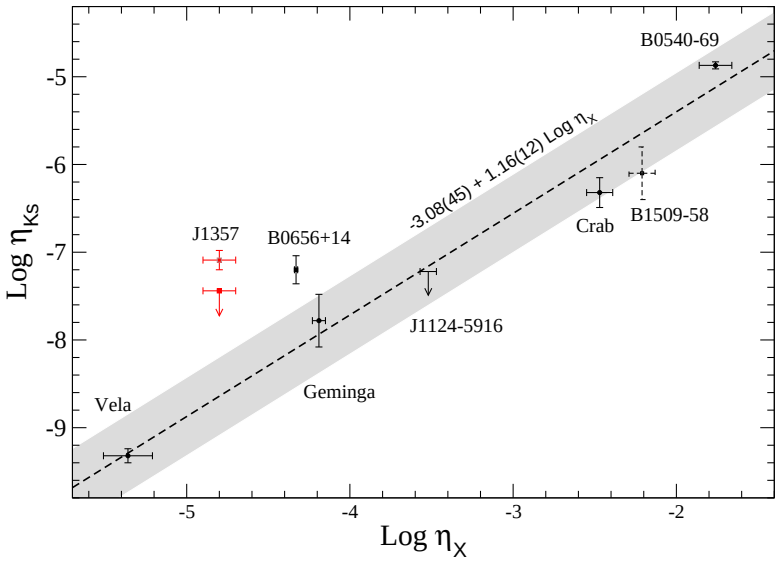

Figure 5. K_s vs. X-ray efficiencies for pulsars observed in both ranges. The dashed line and grey region show the best fit and its 1σ uncertainty to the data for four firmly detected near-IR pulsars (marked by black circles) excluding B0656+14. PSR J1357−6429 is represented by the near-IR counterpart candidate C' and by the detection limit of our observations.

4. Conclusions

We analysed the new radio and near-IR observations of PSR J1357−6429. Based on the new and archival radio-interferometric data, we did not detect any proper motion of the pulsar and estimated the upper limit on its transverse velocity $v_{tr} \lesssim 1300$ km s^{-1} for the distance of 2.5 kpc. The new radio-interferometric position implies that the optical counterpart candidate reported before [7] can now be disclaimed. However, we propose another candidate for the pulsar J1357−6429 counterpart detected in the near-IR. The candidate position overlaps with the new radio-interferometric position of the pulsar. Optical observations of PSR J1357−6429 field using high spatial resolution imaging instruments, like the *Hubble Space Telescope*, would be useful to verify the pulsar nature of the object C'. Further proper motion measurements in the radio and near-IR would be also valuable.

Acknowledgments

The work was supported by the Russian Science Foundation, grant 14-12-00316. The Australia Telescope Compact Array is part of the Australia Telescope National Facility which is funded by the Commonwealth of Australia for operation as a National Facility managed by CSIRO.

References

[1] Camilo F, Manchester R N, Lyne A G, Gaensler B M, Possenti A, D'Amico N, Stairs I H, Faulkner A J, Kramer M, Lorimer D R, McLaughlin M A and Hobbs G 2004 *ApJL* **611** L25–L28
[2] Chang C, Pavlov G G, Kargaltsev O and Shibanov Y A 2012 *ApJ* **744** 81
[3] Esposito P, Tiengo A, de Luca A and Mattana F 2007 *A&A* **467** L45–L48
[4] Lemoine-Goumard M, Zavlin V E, Grondin M H, Shannon R, Smith D A, Burgay M, Camilo F, Cohen-Tanugi J, Freire P C C, Grove J E, Guillemot L, Johnston S, Keith M, Kramer M, Manchester R N, Michelson P F, Parent D, Possenti A, Ray P S, Renaud M, Thorsett S E, Weltevrede P and Wolff M T 2011 *A&A* **533** A102
[5] Zavlin V E 2007 *ApJ* **665** L143–L146
[6] HESS Collaboration 2011 *A&A* **533** A103
[7] Danilenko A, Kirichenko A, Mennickent R E, Pavlov G, Shibanov Y, Zharikov S and Zyuzin D 2012 *A&A* **540** A28
[8] Mignani R P, Shearer A, de Luca A, Moran P, Collins S and Marelli M 2011 *A&A* **533** A101
[9] Kirichenko A, Shibanov Y, Shternin P, Johnston S, Voronkov M A, Danilenko A, Barsukov D, Lai D and Zyuzin D 2015 *MNRAS* **452** 3273–3280
[10] Zyuzin D, Zharikov S, Shibanov Y, Danilenko A, Mennickent R E and Kirichenko A 2016 *MNRAS* **455** 1746–1750
[11] Sault R J, Teuben P J and Wright M C H 1995 *Astronomical Data Analysis Software and Systems IV* (*Astronomical Society of the Pacific Conference Series* vol 77) ed Shaw R A, Payne H E and Hayes J J E p 433
[12] Shibanov Y A, Zharikov S V, Komarova V N, Kawai N, Urata Y, Koptsevich A B, Sokolov V V, Shibata S and Shibazaki N 2006 *A&A* **448** 313–326
[13] Durant M, Kargaltsev O and Pavlov G G 2011 *ApJ* **743** 38